Estimation of nanoparticle's surface electrostatic potential in solution using acid-base molecular probes III: Experimental hydrophobicity/hydrophilicity and charge distribution of MS2 virus surface

Natalya Vodolazkaya[1*], Marina Nikolskaya[1], Anna Laguta[1], Vladimir Farafonov[1], Zita Balklava[2], Michael Stich[3,4], Nikolay Mchedlov-Petrossyan[1], Dmitry Nerukh[3]

[1] Physical Chemistry Department, V.N. Karazin Kharkiv National University, Svoboda Sq. 4, Kharkiv, 61022, Ukraine; [2] College of Health and Life Sciences and [3] Department of Mathematics, Aston University, Birmingham, B4 7ET, UK; [4] Departamento de Matemática Aplicada, Ciencia e Ingeniería de Materiales y Tecnología Electrónica, Universidad Rey Juan Carlos, 28933 Móstoles (Madrid), Spain

ABSTRACT

MS2 bacteriophage is often used as a model for evaluating pathogenic viruses' behaviour in aqueous solution. However, the questions of the virus surface's hydrophilic/hydrophobic balance, the charge distribution, and the binding mechanism are open. Using dynamic light scattering method and laser Doppler electrophoresis the hydrodynamic diameter and the ζ-potential of the virus particles were measured at their concentration of 5×10^{11} particles per mL and ionic strength 0.03 M. The values were found to be 30 nm and –29 or –34 mV (by Smoluchowski or Ohshima approximations) respectively. MS2 bacteriophage surface was also investigated using a series of acid-base indicator dyes of various charge type, size, and structure. Their spectral and acid-base properties (pK_a) are very sensitive to microenvironment in aqueous solution including containing nano-particles. The electrostatic potential of the surface Ψ was estimated using the common formula: $\Psi = 59\times(pK_a^i - pK_a)$ in mV at 25 °C. The Ψ values were –50 mV and +10 mV respectively, which indicate the 'mosaic' way of the charge distribution on the surface. These data are in good agreement with the obtained zeta-potential values and provide even more information about the virus surface. It was found that the surface of the MS2 virus is hydrophilic in solution in contrast to commonly accepted hypothesis of hydrophobicity of virus particles. No hydrophobic interactions between various molecular probes and the capsid were observed.

* Corresponding author. *E-mail address*: vodolazkaya@karazin.ua (N. Vodolazkaya)

Keywords: MS2 virus; bacteriophage; vis-spectroscopy; dynamic light scattering; 'apparent' dissociation constant; surface electrostatic potential; indicator dye; molecular probe; hydrophobicity; charge distribution on MS2 virus surface; size and zeta-potential of MS2 virus.

1. Introduction

The aim of the present investigation was to analyse using physical chemistry approaches (i) the behaviour of MS2 virus particles solution as a colloid system, (ii) their surface properties using several acid-base indicator dyes as molecular probes of various charge type, size and structure, and (iii) the location of the surface bound probes and the charge distribution on MS2 surface.

MS2 is an icosahedral bacteriophage infecting Gram-negative bacteria (*Escherichia coli*) [1-4] and consisting of a protein outer layer (capsid) and encapsulated internal 3569 nucleotides long single stranded RNA genome partly bound to the capsid [5-7]. The capsid protects the genomic RNA, it consists of one maturation protein and 178 copies of the coat protein (arranged as 89 dimers), which self-organise in a shell structure forming the capsid. It is known that the diameter of the capsid is approximately 28 nm and its thickness is about 2.5 nm. The capsid has pores in its wall of the diameter about 1.1 nm [8].

Bacteriophage MS2 is used as a quantitative marker for the effectiveness of antiviral and antiseptic agents, and the efficiency of water treatment plants and filtration devices. Additionally, genetically modified forms of MS2 are available for vaccine development and for use as clinical diagnostic tools [7, 9, 10].

It is reported that MS2, Phi X 174, and PRD1 bacteriophages are commonly used as surrogates to evaluate pathogenic virus behaviour in natural aquatic media [11]. The respective electrostatic and hydrophobic/hydrophilic features of the phages are further shown to be consistent with their measured adhesions onto polyethersulfone-based membranes with distinct hydrophobicities and charge levels. Reported isoelectric point (IEP) is about 2.2–3.9 for MS2 phage [11], and this was confirmed by our experiment too. In the pH range 2–7 at 1 mM, 10 mM and 100 mM $NaNO_3$ concentrations MS2 phage is isolated at pH > 4 with a mean diameter of 27.2 ± 1.5 nm. At pH ≤ 4 MS2 particles are not stable against aggregation. With decreasing pH from 7 to 4, particles come close to each other following a reduction of their electrostatic charge. The electrophoretic mobility of MS2 is systematically negative. The magnitude of the electrophoretic mobility decreases with increasing salt concentration as a result of the screening of the virus charge by the ions present in the electrolytic medium. The mobility of all phages tends to a non-zero plateau value for solution

with ionic strengths above 100 mM which is characteristic of the soft electrokinetic nature of the viruses [11].

From the colloid chemistry point of view MS2 virus particles in solution can be attributed to lyophilic colloidal system. They are formed spontaneously through self-assembling process. The main characteristics of such solutions are as follows: (i) the dispersed phase particles that have strong affinity for the dispersion medium due to the formation of a large number of hydrogen bonds; (ii) being reversible; (iii) being rather stable, they cannot be coagulated easily. However, it is demonstrated experimentally and computationally that non-enveloped viruses are more hydrophobic than a panel of model proteins [12] and that MS2 virus was found highly hydrophobic, evidenced by the microbial adhesion to hydrocarbon hydrophobicity and significantly enhanced adsorption to hydrophobic sand, whereas rotaviruses are relatively hydrophilic [13].

The results of papers [14, 15] demonstrate that MS2 phage expresses relatively low hydrophobicity, but they also provide new data on MS2 hydrophobicity through comparison between native and heated phages. The adhesion experiments showed that 60 °C heat treatment leads to an increase in the hydrophobicity of the remaining infectious MS2 phages compared to the native infectious phages. Non-infectious phages had low hydrophobicity like native phages. At 72 °C, the particles were disrupted, and the genome becomes accessible to RNase. The mean size of MS2 phages did not change at 60 °C compared to the native phages (22 ± 1 nm) but increased at 72 °C to 37 ± 4 nm [14, 15].

It is noted [16] that in 1 : 1 electrolyte solutions (LiCl, NaCl, and KCl), the aggregation of MS2 could not be induced within a reasonable kinetic time frame, and MS2 was stable even at salt concentrations greater than 1.0 M. The aggregation of MS2 could be induced by 2 : 1 electrolytes when Ca^{2+} was employed. Even at Ca^{2+} concentrations as high as 200 mM, diffusion-controlled aggregation was never achieved [16]. In our present investigation this is also confirmed.

Increasing the ionic strength decreased both the inactivation and the capsid breakup in the feed suspension and increased the loss of infectivity in the filtration retentate, while the number of MS2 genomes was identical in both experiments [17].

The work [18] is the first study on toxicity of nanoparticles AgNPs on MS2 bacteriophage. The study shows that both synthesised AgNPs and cultivated MS2 are in nano-size range (27.5±0.4 nm) and exhibit negative surface charge –(26.8±0.8 mV).

The electrophoretic mobility of the MS2 virus measured at various ionic strength levels and pH values were interpreted on the basis of a theoretical formalism [19]. It was shown that the electrokinetic features of MS2 to a large extent determined not only by the external protein capsid but also by the chemical composition and hydrodynamic flow permeation of/within the inner

RNA-protein bound layer and bulk RNA part of the bacteriophage. The impact of virus aggregation, as revealed by decreasing diffusion coefficients for decreasing pH values, was also discussed [19].

MS2 bacteriophage is often used as a model for evaluating pathogenic viruses' behaviour in aqueous solution. However, until recently the problems of the virus surface (i) hydrophilic/hydrophobic balance, (ii) charge distribution, and (iii) the binding mechanism of various probes are open and discussed. Therefore, in the present paper we employ an additional method to investigate the bacteriophage surface using a series of molecular probes (indicator dyes) of various charge type, size, and structure. Their spectral and acid-base properties are very sensitive to microenvironment in aqueous solution including containing nanoparticles.

The key characteristic of a pH-dependent indicator dye H_jR^z dissolved in media containing nanoparticles is the so-called 'apparent' dissociation constant, pK_a^a, as defined by equation (1) [20]:

$$pK_a^a = pH_w + \log\frac{[H_jR^z]}{[H_{j-1}R^{z-1}]}, \quad (1)$$

where the ratio of equilibrium concentrations of H_jR^z and $H_{j-1}R^{z-1}$ is determined UV-Vis spectroscopically; the pH_w values utilised in calculations characterise only the bulk phase and are as a rule measured with a glass electrode. Hence, pK_a^a is an 'instrumental' parameter which can be observed as a constant of two-phase equilibrium between bulk phase and nanoparticle surface. In general case, some fractions of indicator species can stay in the bulk phase. To ensure complete binding, ionic indicators with charge opposite to that of particles surface can be used.

According to the electrostatic theory the apparent value pK_a^a of an indicator under conditions of complete binding of the indicator couple by nanoparticles in solution depends on the transfer activity coefficients, γ_i, and the electrostatic potential of surface [20]:

$$pK_a^a = pK_a^w + \log({}^w\gamma^m_{H_{j-1}R^{z-1}} / {}^w\gamma^m_{H_jR^z}) - \Psi F/(2.303RT) \ . \quad (2)$$

Here pK_a^w is the pK_a value in water; γ_i are the transfer activity coefficients of the corresponding species from water to the surface; ψ is the electrostatic potential of particles surface where molecular probe is located; F is the Faraday constant; R is the gas constant; T is the absolute temperature. The agreed notation of the first two items in the expression for pK_a^a is pK_a^i value so called 'intrinsic' constant. The physical meaning of pK_a^i value can be expressed as pK_a^a value of the molecular probe at $\Psi \to 0$.

Comparing to the values in pure water the following pK_a differences are calculated:

$$\Delta \mathrm{p}K_a^a = \mathrm{p}K_a^a - \mathrm{p}K_a^w = \log({}^w\gamma^m_{\mathrm{H_{j-1}R^{z-1}}} / {}^w\gamma^m_{\mathrm{H_jR^z}}) - \Psi F/(2.303RT), \quad (3)$$

so called medium effect specified by solvation of surface and electrostatic effect [20].

The equation (3) can be transformed into the formula for the estimation of the electrostatic surface potential in mV at 25°C:

$$\psi = 59 \times (\mathrm{p}K_a^i - \mathrm{p}K_a^a). \quad (4)$$

Thus, the aim of the present work is to investigate the physicochemical characteristics of MS2 virus in aqueous solutions, such as hydrodynamic size of the particles, the zeta-potential, the surface potential, hydrophobic/hydrophilic areas of the surface, the stability of MS2 suspension, the biding of molecular probes of various charge type, size and structure, their localisation and the charge distribution on the MS2 surface using dynamic light scattering and spectrophotometric methods, as well as MD.

2. Experimental

2.1. Production and purification of phages

The bacteriophage MS2 (ATCC 15597-B1) and its host *Escherichia coli* (*E. coli*) strain C-3000 (ATCC 15597) were obtained from American Type Culture Collection (ATCC), followed by their propagation, expression and purification as described below. $CaCl_2$ (USP grade), $MgCl_2$ (analytical grade), TRIS (ultrapure) used for the MS2 phage production and purification were from Melford Laboratories, UK. NaCl (analytical grade) was from Duchefa (Netherlands). All chemicals were used without further purification.

Bacteria *E. coli* were cultured in Lennox L Broth medium (Melford Laboratories) at 37 °C and infected with MS2 phage at middle log-phase. After complete lysis of the bacteria, the lysate was centrifuged at 10,000 g for 15 min to remove cell debris, and then centrifuged again at 100,000g at 4 °C for 4 h to pellet the phage particles [21].

The pellet (MS2) was resuspended in buffer containing 50 mM TRIS (pH 7.5), 150 mM NaCl, 5 mM $CaCl_2$, and 5 mM $MgCl_2$. The initial ionic strength of obtained MS2 suspension was 0.18 M.

The working suspensions of MS2 phages were kept at 4 °C before use.

2.2. Infectivity assay

Infectious MS2 phages were enumerated by plaque assay method using the double-agar-layer technique. Ten-fold serial dilutions of the MS2 stock solutions were made to the appropriate dilution in LB medium (for phage enumeration). Infective MS2 phage concentrations were

measured as the number of plaque-forming unit per mL (PFU/mL). The final concentrations of purified phages were 10^{14} PFU/mL and 10^{15} PFU/mL.

The infectivity assay was used for rough estimation of PFU with an error of 10^2. We confirmed that with each step of purification and concentration the PFU increased confirming the presence of concentrated and viable phage.

The MS2 amount (the sample where concentration $\approx 10^{14}$ PFU/mL) was also quantified using the Lowry method and expressed in mg protein per ml [21, 22]. The total protein concentration revealed by this method was 16.5±0.6 mg/ml. The estimated total molecular weight of a single MS2 is 3.6×10^6 g/mol [9].

2.3. Materials, procedure and methods

The samples of the indicator dyes were of high-purity grade. The standard aqueous solution of NaOH was prepared using CO_2-free water and kept protected from the atmosphere. Sodium chloride, aqueous hydrochloric, phosphoric and acetic acids, and borax were of analytical grade.

Suitable pH values of the working solutions used for Vis-spectroscopic pK_a^a measurements were provided by acetate, phosphate, and borate buffers. Hydrochloric acid was used to prepare solutions of pH ≤ 3.5. Stock solutions of the dyes were prepared using water as solvent. All solutions were prepared with double distilled water (18.2 MOhm×cm at 25°C).

All experiments were conducted in the pH range 3–8 to prevent particle aggregation. Thus, the probes were selected such that their pK_a were in this pH range.

The working solutions for pK_a^a measurements were prepared by mixing in 10 mL volumetric flask appropriate aliquots of indicator dyes, buffer components, sodium chloride to keep constant ionic strength (0.03 M) and 0.05 mL MS2 suspension (200 times dilution, 5×10^{11} PFU/mL).

The Vis-absorption spectra were measured using Hitachi U-2000 spectrophotometers against solvent blanks. The pH measurements with the standard deviation of ±(0.01–0.02) were performed using an ESL-63-07 glass electrode and an Ag/AgCl reference electrode in a cell with liquid junction (1 M KCl) at 25.0 ± 0.1 °C, using potentiometer P 37-1; a pH-meter pH-121 served as a nil-instrument. The cell calibration was performed using standard buffers (pH 1.68, 4.01, 6.86, and 9.18) at 25 °C.

2.4. Size and electrophoretic mobility (zeta-potential) measurements

The measurements of MS2 hydrodynamic size and zeta-potential were performed at 25 °C by dynamic light scattering (DLS) method and laser Doppler electrophoresis using Zetasizer Nano

ZS analyzer (Malvern Instruments, He–Ne red laser, wavelength 633 nm, UK), equipped with Dispersion technology and light scattering software.

In Zetasizer Nano ZS 2 different algorithms are used to analyse the correlation function G(τ) of the scattered intensity. These are the cumulants analysis and the distribution analysis. The cumulants analysis is actually a single exponential fit to the autocorrelation function, it gives the value of the polydispersity index (PdI) as a criterion for the width of the distribution, but it does not give the size distribution, and the Z average (the intensity weighted mean hydrodynamic size of the ensemble collection of particles). The calculations for these parameters are defined in the ISO standard document 13321 and 22412. The distribution analysis uses a multiple exponential to fit the correlation function to obtain the distribution of particle sizes and it does not provide the value of the PdI. In this method, PdI is not necessary because the obtained distributions based on the number of peaks can be used to estimate the polydispersity of the system.

Regarding the scattering angle, Malvern took into account all the points that could be associated with this. The Zetasizer Nano ZS measures the intensity of scattered light at an angle of 173° due to conventional factors row.

The viral concentration used in these experiments ranged from ~ 5×10^{11} to 5×10^{12} PFU/mL to obtain strong enough signal from the Zetasizer instrument. Generally, the solutions were not filtered prior to use. However, we conducted special experiments of size and zeta-potential measurements to be sure that no difference was detected between the filtered and not filtered samples for DLS measurements where the solutions, were filtered through a 0.22 μm nylon membrane syringe filter. For size and electrophoretic mobility (zeta-potential) measurements were obtained by means of three independent experiments with triplicate or more measures in each to ensure reproducibility of the measurements.

3. Results and discussion

3.1. The measurements of MS2 size and zeta-potential by DLS method

The main characteristics of colloidal particles in solutions are their size and surface potential, in particular, the zeta-potential, as they allow to predict the kinetic and aggregative stability of the systems, the coagulation process, the substrate binding by surface, etc. To date such information for different kinds of colloidal particles is available for many systems, however the knowledge on the size and zeta-potential of biological nanoparticles, such as viruses, is much less complete. In the following we present the investigation of these parameters using DLS method.

The velocity of particles when an electric field is applied across an electrolyte solution depends on the following factors: (1) the strength of the electric field or the voltage gradient; (2) the dielectric constant of the medium; (3) the viscosity of the medium; (4) the zeta-potential.

The velocity of a particle in an electrical field is commonly referred to as its electrophoretic mobility. The zeta-potential of the particle can be obtained using an equation, which was proposed initially in a complete form by Henry and later expressed by Ohshima in the following form [23]:

$$U_E = \frac{2\varepsilon_r \varepsilon_0 \zeta f(\kappa r)}{3\eta}, \quad (5)$$

where ζ is the zeta-potential, U_E is electrophoretic mobility, ε is dielectric constant, η is viscosity, $f(\kappa r)$ is the Henry's function, where κ is the Debye length ($\kappa = \sqrt{2F^2 I/\varepsilon_0\, \varepsilon_r RT}$), r is the radius of the colloidal particle. If the ionic strength, *I*, in mole per liter, then $\kappa = 3.299\sqrt{I}$, nm^{-1}. f as a function of $\kappa \times r$ can be written as

$$f = 1 + 0.5\left[1 + \frac{2.5}{\kappa r[1 + 2\exp(-\kappa r)]}\right]^{-3}. \quad (6)$$

Two constants are generally used as approximations for the value of f, 1.5 or 1.0 [24]. In aqueous media and moderate electrolyte concentrations f approximated to 1.5 is referred to as Smoluchowski approximation. Therefore, the calculation of the zeta-potential from the mobility is straightforward for the systems that fit the Smoluchowski model, i.e., with particles larger than ~0.2 microns dispersed in electrolytes containing over 10^{-3} molar salts. For small particles in low dielectric constant media f is assumed to be 1.0 that allows equally simple calculations. This is referred to as Hückel approximation, typical for non-aqueous systems.

However, a more precise model should have the κr dependence of f. For example, the Ohshima approximation at constant ionic strength of aqueous solutions and various particles size or at constant particles size and various ionic strength, 25 °C:

κr	0.1	0.5	1	2	5	10	20	25	50	100	500
f	1.001	1.014	1.034	1.064	1.15	1.25	1.35	1.38	1.43	1.46	1.49

We have used all three approximations for the calculation of the zeta-potential from the DLS data. Below we demonstrate the difference in obtained results and the optimal zeta-potential values.

3.1.1. MS2 sample with 10^{14} pfu concentration obtained by usual centrifugation

50, 100, 200, and 400-fold dilution of the MS2 initial suspension did not change the hydrodynamic size of individual particles and aggregates. The average diameter (±5 nm in all

cases) was on the first peak 30 nm by intensity; 20 nm by volume; 20 nm by number and on the second peak 300–400 nm by intensity; 500 nm by volume respectively (Fig. 1, Table 1).

When the solution was filtered before the measurement, individual MS2 particles were detected by DLS method, but not aggregates. After one day, the results were reproducible for the solutions at all dilutions. After two weeks individual particles were not dominated, but their size was the same as for freshly prepared solutions. The size of the aggregates was increasing until 900 nm, becoming the largest peak by intensity.

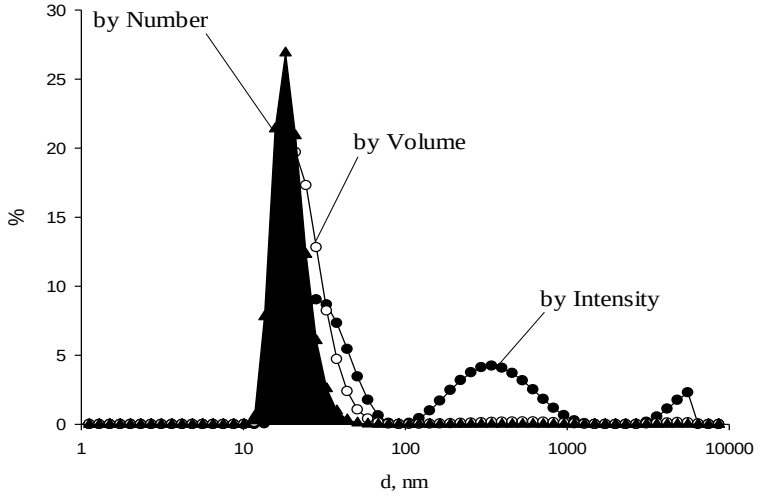

Fig 1. Size distribution by number, volume, and intensity of MS2 solution at the concentration of 5×10^{11} virus particles per mL (200-fold dilution) and 0.03 M ionic strength (NaCl)

Table 1. The hydrodynamic diameter of MS2 particles at various dilution of the initial suspension (10^{14} pfu concentration) and polydispersity index, PdI (average PdI value lies in the range 0.08 ÷ 0.7) at 25 °C

Dilution of MS2 suspension	Ionic strength of solution / M	Diameter / nm				
		by intensity		by volume	by number	PdI
		I Peak	II Peak			
1/50	3.6×10^{-3}	35 ± 1	440 ± 6	25 ± 1	20 ± 1	0.56 ± 0.01
1/100	1.8×10^{-3}	34 ± 1	380 ± 5	25± 1	21 ± 1	0.5 ± 0.1
1/200	9×10^{-4}	33 ± 2	340 ± 4	25 ± 1	21 ± 1	0.53 ± 0.09
1/400	4.5×10^{-4}	36 ± 2	210 ± 4	28 ± 1	23 ± 1	0.68 ± 0.07

The electrophoretic mobility of particles in 50, 100, 200, and 400-fold diluted MS2 initial suspension is presented in Table 2 and Fig. 2. The calculations of the zeta-potential were carried out at f = 1.5 (the Smoluchowski model); f = 1 (the Hückel equation) and f calculated using the approximation proposed by Ohshima (Table 2). The zeta-potential of the MS2 solutions was also obtained at 200-fold dilution (5×10^{11} particles per mL) and 0.03 M ionic strength (buffer solutions

components of initial MS2 suspension and NaCl). The total ionic strength of 0.03 M was chosen because we also determined pK_a values of the indicator dyes to estimate the MS2 surface potential for which the minimal constant ionic strength in solution at pH variation had to be 0.03 M. This means that for correct comparison of the zeta-potential and the estimated surface potential from pK_a values they should be at the same ionic strength. Well reproducible values of the zeta-potential of individual particles were obtained (±3 mV): –29 mV (f = 1.5), –39 mV (f = 1), and –34 mV (variable f) (Fig. 2). It is necessary to note that in the calculation of the zeta-potential values using electrophoretic mobility measured by Zetasizer, the influence of the ionic strength of the solution as well as other parameters of the investigated systems should be taken into account according to the IUPAC recommendations [23]. Namely, the Henry equation must be applied with the approximation proposed by Ohshima. The Smoluchowski approximation as recommended in the Zetasizer manual gives too approximate results in most cases for various systems, especially in the aqueous solutions of phages. It is, however, a widely used practice reported in literature for similar systems. The second case at f = 1 is not appropriate because it was calculated for small particles in low dielectric constant media model, which is not our case. The third case (variable f) is closer to reality because it takes into consideration the influence of the salt on the double electric layer of the surface. Note, that on the curve of the zeta-potential distribution the second peak is observed at ~ –(9 ± 2) mV. This value corresponds to the abovementioned MS2 aggregates with definite size.

Table 2. ζ-Potential values (±3 mV) and electrophoretic mobility (±0.1 μmcm/Vs) of MS2 particles in aqueous solution (initial concentration 10^{14} pfu) at various dilution of the initial suspension at 25 °C

Dilution of MS2 suspension	Ionic strength of solution / M	Electrophoretic mobility / μmcm/Vs		ζ / mV by Smoluchowski (f = 1.5)		ζ / mV by Hückel (f = 1)		ζ / mV by Ohshima (variable f)	
		I Peak	II Peak	I Peak	II Peak	I Peak	II Peak	I Peak	II Peak
1/50	3.6×10^{-3}	–0.3	–1.9	–3	–24	–5	–36	–5	–32
1/100	1.8×10^{-3}	–0.4	–2.0	–5	–26	–8	–39	–7	–36
1/200	9×10^{-4}	–0.4	–2.1	–5	–27	–8	–40	–7	–37
1/400	4.5×10^{-4}	–0.8	–2.4	–10	–31	–15	–46	–14	–44

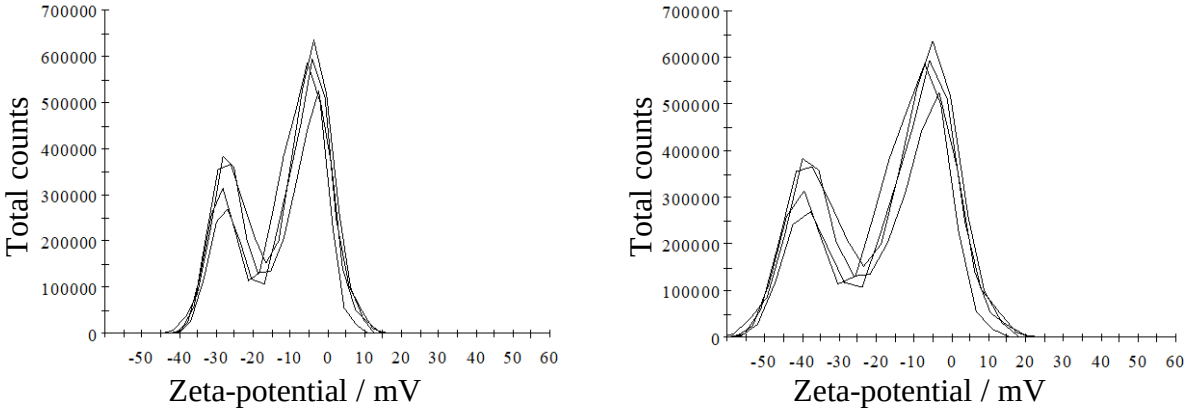

Fig 2. Zeta-potential distribution of MS2 aqueous solution at the concentration of 5×10^{11} virus particles per mL (200-fold dilution) using Smoluchowski (***a***) and Ohshima (***b***) approximations, 9×10^{-4} M ionic strength

The ionic strength of MS2 solution (5×10^{11} particles per mL) was varied by NaCl from 9×10^{-4} to 0.8 M. Varying the salt concentration in wide limits did not change the hydrodynamic particles size significantly (Fig. 3). The hydrodynamic diameter of individual particles for all NaCl concentration was 30 nm by intensity; 25 nm by volume; 20 nm by number. The size of the aggregates was ~600 nm by intensity; ~700 nm by volume (Table 3). After two weeks the size of the aggregates in the same solutions increased to ~900 nm, but individual particles were also recorded with the size of ~30 nm.

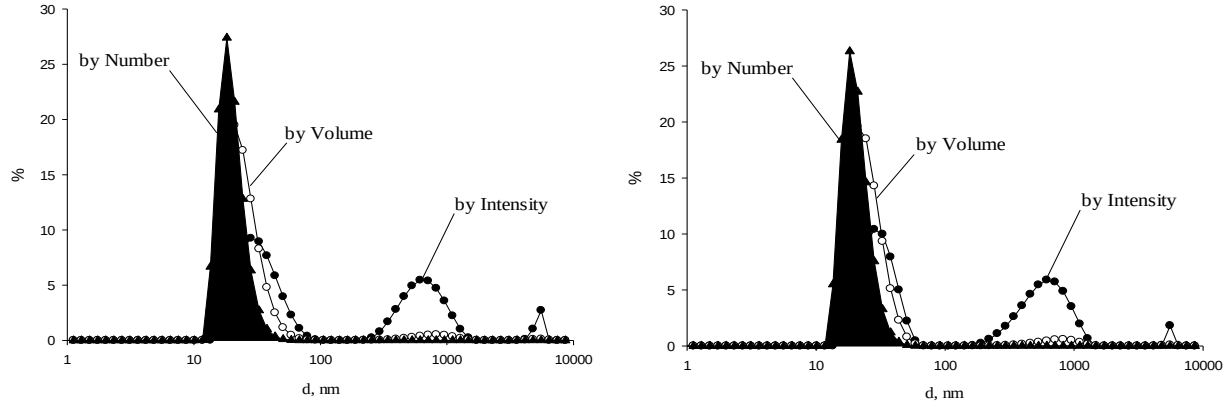

Fig 3. Size distribution by number, volume and intensity of MS2 solution at concentration 5×10^{11} virus particles per mL (200-fold dilution) and ionic strength (***a***) 0.1 M (NaCl) and (***b***) 0.8 M (NaCl)

Table 3. The diameter of MS2 particles at varying ionic strengths (5×10^{11} particles per mL, 200-fold dilution) and polydispersity index, PdI (average PdI value lies in the range 0.08 ÷ 0.7) at 25 °C

c(NaCl) / M	Diameter / nm				PdI
	by intensity		by volume	by number	
	I Peak	II Peak			
0	33 ± 2	340± 4	25 ± 1	21 ± 1	0.53 ± 0.09
0.03	33 ± 1	290 ± 8	25 ± 1	21 ± 1	0.64 ± 0.03
0.06	32 ± 1	310 ± 3	25 ± 1	21 ± 1	0.66 ± 0.09
0.1	30 ± 1	500 ± 1	24 ± 1	20 ± 1	0.48 ± 0.09
0.2	30 ± 1	800 ± 1	25 ± 1	22 ± 1	0.51 ± 0.06
0.3	30 ± 1	500 ± 1	24 ± 1	21 ± 1	0.52 ± 0.09
0.8	30 ± 1	700 ± 2	24 ± 1	21 ± 1	0.53 ± 0.09

For the zeta-potential measurements at varying ionic strength and expected double electrical layer compression we obtained the following results. In the range of NaCl concentration from 0.06 to 0.8 M only one peak was recorded on the distribution curve ~ –9 mV (Fig. 4). We relate this peak to MS2 aggregates of 600 nm size, but the first peak at ~ –35 mV at 0–0.03 M NaCl concentrations corresponded to individual particles disappeared. However, at the same time, the size distribution shows clearly both peaks at this ionic strength. In the range of NaCl concentration 0÷0.03 M two peaks were present on the size and zeta-potential distribution curves at 30 and 600 nm; –35 and –9 mV respectively (Table 4).

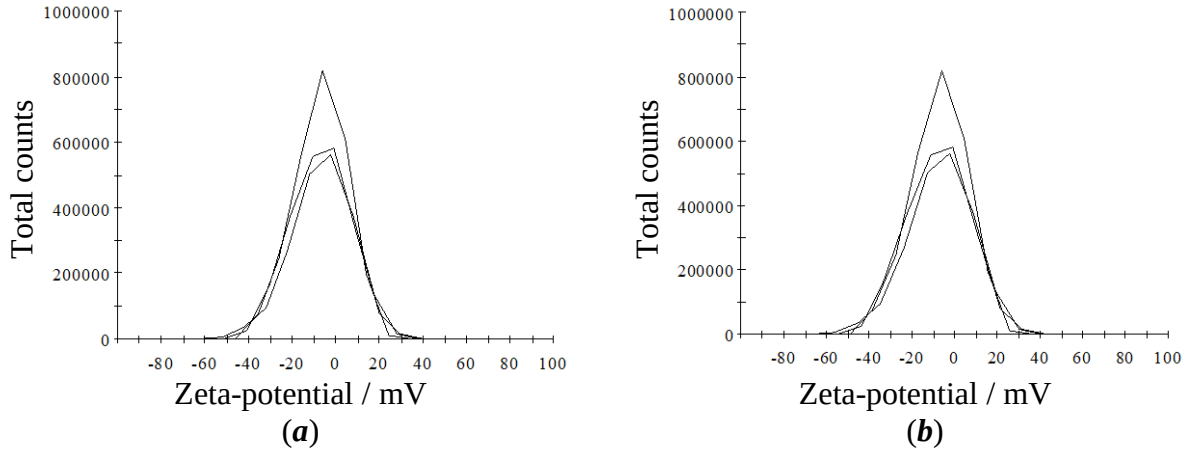

Fig 4. Zeta-potential distribution of MS2 solution at concentration 5×10^{11} virus particles per mL (200-fold dilution) using Smoluchowski (***a***) and Ohshima (***b***) approximations at 0.2 M NaCl

Table 4. ζ-Potential values (±3 mV) and electrophoretic mobility (±0.1 μmcm/Vs) of MS2 particles in solution (initial concentration is 10^{14} pfu) at various ionic strength of MS2 aqueous solution (5×10^{11} particles per mL, 200-fold dilution) at 25 °C

c(NaCl) / M	Electrophoretic mobility / μmcm/Vs		ζ / mV by Smoluchowski (f = 1.5)		ζ / mV by Hückel (f = 1)		ζ / mV by Ohshima (variable f)	
	I Peak	II Peak	I Peak	II Peak	I Peak	II Peak	I Peak	II Peak
0	–0.41	–1.92	–5	–25	–8	–37	–7	–35
0.03	–0.50	–2.10	–6	–29	–10	–39	–7	–34
0.06	–0.61	–	–8	–	–12	–	–9	–
0.1	–0.47	–	–6	–	–9	–	–7	–
0.2	–0.50	–	–6	–	–10	–	–7	–
0.3	–0.50	–	–7	–	–8	–	–7	–
0.8	–0.35	–	–6	–	–7	–	–6	–

3.1.2. MS2 sample with 10^{15} pfu concentration and obtained by ultracentrifugation

50, 100, 200, and 400-Fold dilution of MS2 initial suspension with 10^{15} pfu concentration and subsequent ultracentrifugation did not change the size of individual particles and existing aggregates (average diameter (±5 nm) was 35 nm by intensity; 28 nm by volume; 22 nm by number and 700–800 nm by intensity; 1000 nm by volume respectively) (Fig. 5, Table 5). These results were reproduced three times. There was significant difference (~300–400 nm) in aggregates size compared to MS2 initial suspension with 10^{14} pfu concentration.

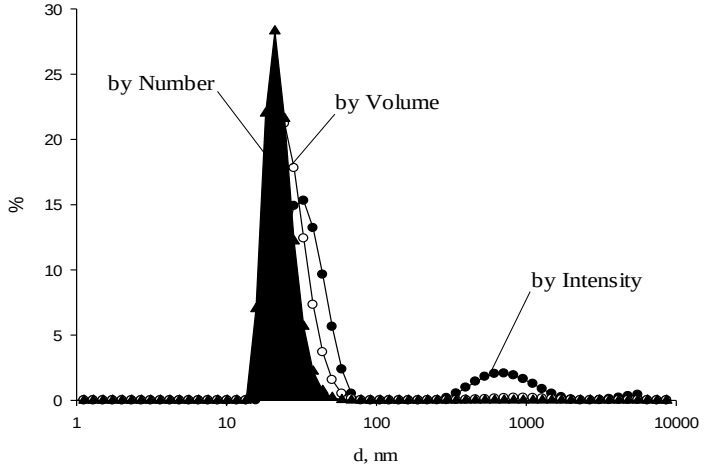

Fig 5. Size distribution by number, volume and intensity of MS2 solution at concentration 5×10^{12} virus particles per mL (200-fold dilution) and ionic strength 0.03 M (NaCl)

Table 5. The diameter of MS2 particles at various dilution of initial suspension (10^{15} pfu concentration) at 25 °C

Dilution of MS2 suspension	Ionic strength of solution / M	Diameter / nm by intensity		by volume	by number	PdI
		I Peak	II Peak			
1/50	3.6×10^{-3}	33 ± 1	700 ± 9	26 ± 1	22 ± 1	0.34 ± 0.01
1/100	1.8×10^{-3}	34 ± 4	900 ± 1	26 ± 1	21 ± 1	0.30 ± 0.01
1/200	9×10^{-4}	34 ± 5	1000 ± 2	27 ± 1	22 ± 1	0.29 ± 0.02
1/400	4.5×10^{-4}	34 ± 1	800 ± 3	27 ± 1	23 ± 1	0.30 ± 0.03

The particles electrophoretic mobility in these systems is presented in Table 6. The calculation of zeta-potential was also carried out according Hückel equation, Smoluchowski model, and variable f by Ohshima equation (Table 6, Fig. 6). Zeta-potential of MS2 particles was also measured at 200-fold dilution (5×10^{12} particles per mL) and ionic strength 0.03 M (buffer solutions components of initial MS2 suspension and NaCl). Well reproducible values of the zeta-potential of individual particles were obtained (±3 mV): –24 mV (f = 1.5) and –29 mV (variable f). However, the second peak (around –9 mV) was not observed as in the case with first sample of MS2 suspension (10^{14} pfu). Probably, because of large MS2 aggregates (~600–800 nm) which have zeta-potential value less than –9 mV and it was not fixed or/and according to the PdI value (Table 5) MS2 aggregates are negligible and it cannot be enough to determine their zeta-potential.

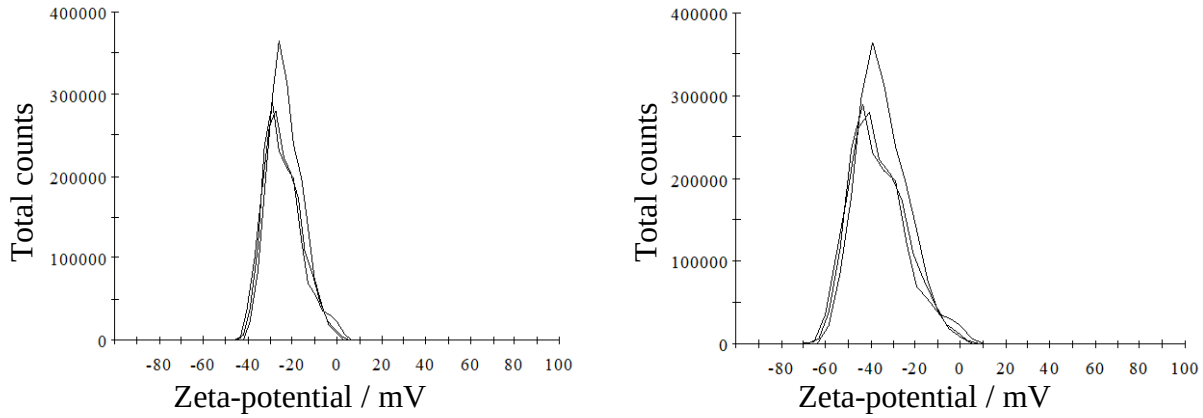

Fig 6. Zeta-potential distribution of MS2 solution at concentration 5×10^{12} virus particles per mL (200-fold dilution) using Smoluchowski (***a***) and Ohshima (***b***) approximations, $I = 9\times10^{-4}$ M

Table 6. ζ-Potential values (±3 mV) and electrophoretic mobility (±0.1 μmcm/Vs) of MS2 particles in solution (initial concentration is 10^{15} pfu) at various dilution of the initial suspension at 25 °C

Dilution of MS2 suspension	Ionic strength of solution / M	Electrophoretic mobility / μmcm/Vs	ζ / mV by Smoluchowski (f = 1.5)	ζ / mV by Hückel (f = 1)	ζ / mV by Ohshima (variable f)
1/50	3.6×10^{-3}	–1.8	–23	–35	–31
1/100	1.8×10^{-3}	–1.8	–23	–35	–32
1/200	9×10^{-4}	–1.9	–24	–36	–34
1/400	4.5×10^{-4}	–2.2	–28	–43	–41

The ionic strength of the MS2 solution (5×10^{12} particles per mL) was varied using NaCl from 9×10^{-4} to 0.8 M. The change of salt concentration in wide limits did not influence significantly the particles size. It was the same value as at 0.03 M NaCl as mentioned above. The measurements of the zeta-potential at variation of NaCl concentration in the range 0÷0.8 M gave opposite result in this case than with the first MS2 sample (Table 4): dramatically decreasing of zeta-potential value after 0.03 M NaCl (Table 7). Probably because of the large MS2 aggregates are absent in given case.

Table 7. ζ-Potential values (±3 mV) and electrophoretic mobility (±0.1 μmcm/Vs) of MS2 particles in solution (initial concentration is 10^{15} pfu) at various ionic strength of MS2 solution (5×10^{12} particles per mL, 200-fold dilution) at 25 °C

c(NaCl) / M	Electrophoretic mobility / μmcm/Vs	ζ / mV by Smoluchowski (f = 1.5)	ζ / mV by Hückel (f = 1)	ζ /mV by Ohshima (variable f)
0	–1.9	–24	–36	–34
0.03	–1.9	–24	–36	–29
0.06	–0.90	–12	–17	–13
0.1	–0.7	–9	–14	–10
0.2	–0.6	–8	–12	–8
0.3	–0.16	–2	–3	–2
0.8	–0.08	–1	–2	–1

The ionic strength of the MS2 solution (5×10^{12} particles per mL) was also varied using $CaCl_2$ from 9×10^{-4} M to 0.01 M. The size of individual particles and existing aggregates were 33 nm by intensity; 27 nm by volume; 23 nm by number and 450 nm by intensity respectively (Fig. 7). The change of salt concentration in wide limits did not influence significantly the size of individual particles, but increased the fraction of MS2 aggregates.

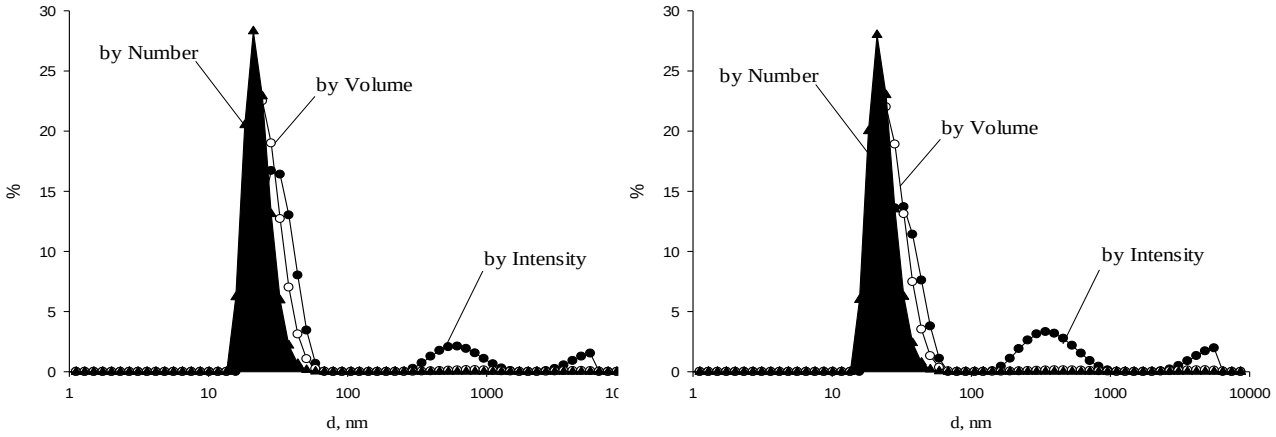

a ***b***

Fig 7. Size distribution by number, volume and intensity of MS2 solution at concentration 5×10^{12} virus particles per mL (200-fold dilution) and ionic strength (***a***) 0.0001 M ($CaCl_2$) and (***b***) 0.01 M ($CaCl_2$)

The influence of $CaCl_2$ salt on the zeta-potential value was predictable because of larger cation charge compared to the one-one electrolyte NaCl. For example, the zeta-potential was about –10 mV at 0.01 M $CaCl_2$ and at 0.1 M NaCl explained by the enhancement of the screening of the surface charge by Ca^{2+}. The results are collected in Table 8.

Table 8. ζ-Potential values (±3 mV) and electrophoretic mobility (±0.1 μmcm/Vs) of MS2 particles in solution (initial concentration is 10^{15} pfu) at various ionic strength of MS2 solution (5×10^{12} particles per mL, 200-fold dilution) at 25 °C

$c(CaCl_2)$ / M	Electrophoretic mobility / μmcm/Vs	ζ / mV by Smoluchowski (f = 1.5)	ζ / mV by Hückel (f = 1)	ζ /mV by Ohshima (variable f)
0	–1.9	–24	–36	–34
1×10^{-4}	–1.8	–23	–35	–33
5×10^{-4}	–0.9	–18	–27	–25
1×10^{-3}	–1.1	–14	–21	–19
5×10^{-3}	–0.7	–9	–13	–12
1×10^{-2}	–0.7	–9	–13	–11

3.2. The investigation of the bacteriophage surface using a series of acid-base probes (indicator dyes). The estimation of electrostatic potential of the MS2 surface Ψ *using* pK_a *values of acid-base probes*

In general, the surface of the virus particles is negatively charged according to the data of laser Doppler electrophoresis, and zeta-potential reflects this. However, acid-base indicator dyes as

molecular probes of various charge type, size, and structure in the solutions containing MS2 particles can be bound by the surface and give precise information about local electrostatic potential. The latter is always higher than the zeta-potential by absolute value. It also provides more detailed information about the surface.

We examined the pK_a values of 12 acid-base probes of various charge type, size, and structure: small anionic (β, γ-dinitrophenols, and *para*-nitrophenol), large cationic (neutral red, hexamethoxy red, rhodamine B, quinaldine red), large cationic as well as solvatochromic and hydrophobic (Standard Reichardt's dye), large anionic (bromothymol blue, ethyl ester of fluorescein), hydrophobic anionic (β-dinitro-4-*n*-dodecylphenol, *n*-decyl ester of fluorescein) in MS2 solution (Table 9). Their spectral and acid-base properties are very sensitive to their microenvironment in aqueous solution [20].

In all cases the maxima of the absorption spectra of indicator dyes in MS2 solutions coincide with those in aqueous solution. This is not typical for molecular probes bound by charged nanoparticles in solutions [20]. However, such behavior can be observed on the surface of nanoparticles, if enough water molecules are absorbed.

The main equations describing the behaviour of molecular probes in solutions containing nanoparticles are given in Introduction (Eq. 1-4). In our case we assume that the molecular probes are completely bound due to electrostatic interactions. However, it is difficult to verify this fact in virus suspensions, in contrast to micellar solutions of surfactants. In the latter it is very easy to vary the micelles concentration and to achieve the constant pK_a values of indicator dyes as evidence of complete binding [20].

Comparing to the pK_a values in pure water the following pK_a differences were calculated ΔpK_a (Eq. 3) (Table 9). On average they were +0.43 for large positive probes and –0.21 for small negative probes. The pK_a values of small and large hydrophobic probes as well as large negative probes did not show any difference in solution with virus and without it, which contradicts the commonly accepted hypothesis of the hydrophobicity areas on the virus surface [12-14]. This provides information on the probes' binding by the virus surface, summarised in Table 10.

Table 9. The pK_a and Δ pK_a of various indicators in MS2 solution at concentration 5×10^{11} virus particles per mL and ionic strength 0.03 M (components of buffer solutions and NaCl), and the estimated ψ value of capsid surface at 25 °C

Type of indicator probe	Indicator / charge type of acid-base couple	pK_a	pK_a^{w*} (±0.05)	ΔpK_a	Estimated ψ/ mV value (±5 mV) from eq. 4
Small anionic (~0.9 nm)	*β*-dinitrophenol (0/–)	3.49±0.05	3.70	–0.21	+12
	γ-dinitrophenol (0/–)	4.95±0.05	5.22	–0.27	+16
	para-nitrophenol (0/–)	7.00±0.05	7.15	–0.15	+9
Large cationic (>1.2 nm)	Neutral red (+/0)	6.77±0.09	6.50	0.27	–60
	Hexamethoxy red (+/0)	3.59±0.07	3.10	0.49	–70
	Rhodamine B (+/±)	3.79±0.05	3.26	0.53	–30
	Quinaldine red (2+/+)	not bound ($pK_a = pK_a^w$)			
Large cationic, solvatochromic and hydrophobic (>1.2 nm)	Standard Reichardt's dye (+/±)	not bound ($pK_a = pK_a^w$)			
Large anionic (>1.2 nm)	Bromothymol blue (–/2–)	not bound ($pK_a = pK_a^w$)			
	Ethyl ester of fluorescein (0/–)	not bound ($pK_a = pK_a^w$)			
Hydrophobic anionic (0.9 and 1.2 nm)	*β*-Dinitro-4-*n*-dodecylphenol (0/–)	not bound ($pK_a = pK_a^w$)			
	n-Decyl ester of fluorescein (0/–)	not bound ($pK_a = pK_a^w$)			

* pK_a^w values of molecular probes were obtained under the same conditions as pK_a values in MS2 solution.

Table 10. Acid-base probes interaction with MS2 particles

	Small probes (~0.9 nm)	Large probes (>1.2 nm)	Hydrophobic probes (0.9 and 1.2 nm)
Cationic form	**not tested**	**bound**	**not bound**
Anionic form	**bound**	**not bound**	**not bound**

The electrostatic potential of the surface, Ψ, can be estimated using the common formula $\Psi = 59\times(pK_a^i - pK_a)$, mV [20]. The p$K_a^i$ value on ionic surface is often equated to the pK_a value of the same indicator bound by nonionic or zwitterionic surface where $\psi \to 0$ or pK_a^w value in water. We estimated the Ψ values of the virus surface by these three approaches. However, the obtained data show that the optimal approximation of the pK_a^i value is the pK_a value of the same indicator

bound by a nonionic surface. The zwitterionic surface has a chameleon-like nature and the surface can be positively or negatively charged, being only in few cases. The approximation of pK_a^i value as pK_a^w value in water is not sufficiently accurate because it does not take into account the transfer activity coefficients (γ_i) of the corresponding species from water to the surface (eq. 2).

The values of ΔpK_a in the virus solutions were positive for positive probes, which is characteristic for negatively charged surfaces (Fig. 8, left) and negative for negatively charged probes (Fig. 8, right) typical for positively charged surfaces [20]. The Ψ values on average were –50 mV and +10 mV respectively (Table 9), which indicates the 'mosaic' way of the charge distribution on the surface (Fig. 9). This mosaic character is evident from the distribution of the charged amino acid residues across the capsid (Fig. 9).

It is important to note that different indicators give positive or negative Ψ values in the same pH range. That is, it is not the effect caused by varying pH, and this is a new result, perhaps requiring additional experiments and thinking.

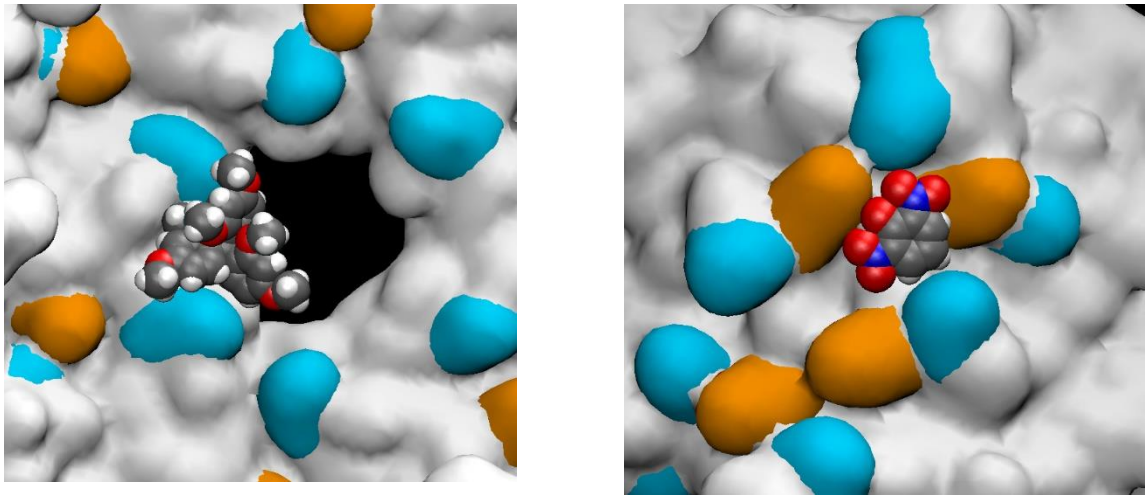

Fig. 8. Schematic assumed localisation of the large positive, hexamethoxy red (left) and small negative, *β*-dinitrophenol (right) probes on the surface of the virus. We emphasize that this is an illustration based on the results of the experiment, not a product of docking or other computational method.

We conclude that the surface of the virus is hydrophilic in solution in contrast to commonly accepted hypothesis of hydrophobicity of virus particles. We found that the overall ζ-potential

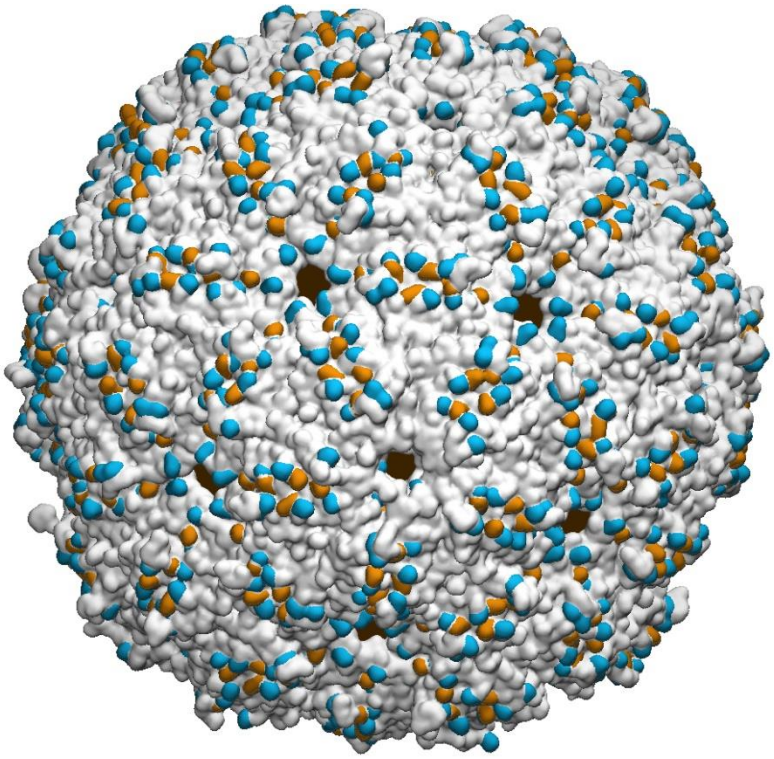

Fig. 9. Mosaic structure of charge distribution, blue – negative (Glu and Asp amino acid residues), orange – positive (Arg and Lys amino acid residues), black – pores. The distribution corresponds to pH ~ 7.

of the virus particle is negative, approximately –30 mV, confirming literature results [18]. However, using acid-base probes we have experimentally detected patches of positive and negative charge on the surface (Fig. 9) and demonstrated their impact on the binding of small molecules to the capsid.

4. Conclusions

We investigated experimentally the bacteriophage surface at physiological conditions estimating its hydrophobicity/hydrophilicity and charge distribution using a series of acid-base molecular probes (indicator dyes).

The hydrodynamic diameter and the zeta-potential of the virus particles were measured at their concentration of 5×10^{11} particles per mL and ionic strength 0.03 M. The values were found to be 30 nm and –29 or –34 mV (by Smoluchowski or Ohshima approximations) respectively using the dynamic light scattering method and laser Doppler electrophoresis.

It was found that the surface of the MS2 virus is hydrophilic in solution in contrast to commonly accepted hypothesis of hydrophobicity of virus particles. No hydrophobic interactions between various molecular probes and the capsid were observed.

The local Ψ values of MS2 particles were examined by molecular probes of various charge type, size, and structure to compare with obtained zeta-potential of the virus particles. It was found using molecular probes, that the local electrostatic potentials of the MS2 surface are –50 mV and +10 mV, which indicate the 'mosaic' way of the charge distribution on the surface confirming our computer simulation results [8, 25].

Acknowledgements

N. M.-P. thanks the Ministry of Education and Science of Ukraine for financial support in the frame of the project #0122U001485. A. L. and V. F. thank the Ministry of Education and Science of Ukraine for financial support in the frame of the project #0120U101064. V. F. and D. N. acknowledge the use of HPC Midlands supercomputer funded by EPSRC, grant number EP/P020232/1; the access to HPC Call Spring 2021, EPSRC Tier-2 Cirrus Service; the access to Sulis Tier 2 HPC platform hosted by the Scientific Computing Research Technology Platform at the University of Warwick. Sulis is funded by EPSRC Grant EP/T022108/1 and the HPC Midlands+ consortium. The authors thank Gorbenko G. P. and her research group (V.N. Karazin Kharkov National University) for the estimation of MS2 amount (the total protein concentration) using the Lowry method.

References

1. Strauss, Jr. J. H.; Sinsheimer, R. L. Purification and Properties of Bacteriophage MS2 and of its Ribonucleic Acid. *J. Mol. Biol.* **1963**, *7*, 43–54. DOI:10.1016/S0022-2836(63)80017-0

2. Hu, B.; Khara, P.; Christie, P. J. Structural Bases for F Plasmid Conjugation and F pilus Biogenesis in Escherichia coli. *Proc. Natl. Acad. Sci. (PNAS).* **2019**. *116,* 14222–14227. DOI: 10.1073/pnas.1904428116

3. Harb, L.; Chamakura, K.; Khara, P.; Christie, P.J.; Young, R.; Zeng, L. ssRNA Phage Penetration Triggers Detachment of the F-pilus. *Proc. Natl. Acad. Sci. (PNAS)*. **2020**. *117,* 25751–25758. DOI:10.1073/pnas.2011901117

4. Wagner, A.; Weise, L. I.; Mutschler, H. In Vitro Characterisation of the MS2 RNA Polymerase Complex Reveals Host Factors that Modulate Emesviral Replicase Activity. *Communications Biology*. **2022**. *5*, 264-275. DOI:10.1038/s42003-022-03178-2

5. Valegard, K.; Liljas, L.; Fridborg, K.; Unge, T. The Three-Dimensional Structure of the Bacterial Virus MS2. *Nature* **1990**, *345*, 36–41. DOI:10.1038/345036a0

6. Machado, M.R.; Pantano, S. Fighting Viruses with Computers, Right Now. *Current Opinion in Virology.* **2021**. *48*, 91–99. DOI: 10.1016/j.coviro.2021.04.004

7. Le, D.T.; Müller, K.M. In Vitro Assembly of Virus-Like Particles and Their Applications. *Life*. **2021**. *11*, 334-353. DOI: 10.3390/life11040334

8. Farafonov, V.; Nerukh, D. MS2 Bacteriophage Capsid Studied Using All-Atom Molecular Dynamics. *Interface Focus* **2019**, *9*, 20180081. DOI:10.1098/rsfs.2018.0081

9. Kuzmanovic, D. A.; Elashvili, I.; Wick, Ch.; O'Connell, C.; Krueger, S. Bacteriophage MS2: Molecular Weight and Spatial Distribution of the Protein and RNA Components by Small-Angle Neutron Scattering and Virus Counting. *Structure* **2003**, *11*, 1339–1348. DOI:10.1016/j.str.2003.09.021

10. Fu, Y.; Li, J. A Novel Delivery Platform Based on Bacteriophage MS2 Virus-Like Particles. *Virus Res.* **2016**, *211*, 9–16. DOI:10.1016/j.virusres.2015.08.022

11. Dika, Ch.; Duval, J., F. L.; Francius, G.; Perrin, A.; Gantzer, Ch. Isoelectric Point is an Inadequate Descriptor of MS2, Phi X 174 and PRD1 Phages Adhesion on Abiotic Surfaces. *J. Colloid Interface Sci.* **2015**, *446*, 327–334. DOI:10.1016/j.jcis.2014.08.055

12. Heldt, C. L.; Zahid, A.; Vijayaragavan, S. K.; Mi, X. Experimental and Computational Surface Hydrophobicity Analysis of a Non-Enveloped Virus and Proteins. *Colloids Surf. B* **2017**, *153*, 77–84. DOI:10.1016/j.colsurfb.2017.02.011

13. Farkas, K.; Varsani, A.; Pang, L. Adsorption of Rotavirus, MS2 Bacteriophage and Surface-Modified Silica Nanoparticles to Hydrophobic Matter. *Food Environ Virol* **2015**, *7*, 261–268. DOI:10.1007/s12560-014-9171-3

14. Brié, A.; Bertrand, I.; Meo, M.; Boudaud, N.; Gantzer, Ch. The Effect of Heat on the Physicochemical Properties of Bacteriophage MS2. *Food Environ Virol* **2016**, *8*, 251–261. DOI:10.1007/s12560-016-9248-2

15. Dika, C.; Ly-Chatain, M. H.; Francius, G.; Duval, J. F. L.; Gantzer, C. Non-DLVO Adhesion of F-specific RNA Bacteriophages to Abiotic Surfaces: Importance of Surface Roughness, Hydrophobic and Electrostatic Interactions. *Colloids Surf. A* **2013**, *435*, 178–187. DOI:10.1016/j.colsurfa.2013.02.045

16. Mylon, S. E.; Rinciog, C. I.; Schmidt, N.; Gutierrez, L.; Wong, G. C. L.; Nguyen, Th. H. Influence of Salts and Natural Organic Matter on the Stability of Bacteriophage MS2. *Langmuir* **2010**, *26*, 1035–1042. DOI:10.1021/la902290t

17. Furiga, A.; Pierre, G.; Glories, M.; Aimar, P.; Roques, Ch.; Causserand, Ch.; Berge, M. Effects of Ionic Strength on Bacteriophage MS2 Behavior and Their Implications for the Assessment of Virus Retention by Ultrafiltration Membranes. *Appl. Environ. Microbiol.* **2011**, *77*, 229–236. DOI:10.1128/AEM.01075-10

18. Shao, F. Toxicity of Silver Nanoparticles on Virus. *J. Mater. Environ. Sci.* **2014**, *5*, 587–590.

19. Langlet, J.; Gaboriaud, F.; Gantzer, C.; Duval, J. F. Impact of Chemical and Structural Anisotropy on the Electrophoretic Mobility of Spherical Soft Multilayer Particles: the Case of Bacteriophage MS2. *Biophysical J.* **2008**, *94*, 3293–3312. DOI:10.1529/biophysj.107.115477

20. Mchedlov-Petrossyan, N. O.; Vodolazkaya, N. A.; Gurina, Yu. A.; Sun, W.-C.; Gee, K. R. Medium Effects on the Prototropic Equilibria of Fluorescein Fluoroderivatives in True and Organized Solution. *J. Phys. Chem.* **2010**, *114*, 4551–4564. DOI:10.1021/jp909854s

21. Vus, K.; Tarabara, U.; Balklava, Z.; Nerukh, D.; Stich, M.; Laguta, A.; Vodolazkaya, N.; Mchedlov-Petrossyan, N.; Farafonov, V.; Kriklya, N.; Gorbenko, G.; Trusova, V.; Zhytniakivska, O.; Kurutos, A.; Gadjev, N.; Deligeorgiev, T. Association of Novel Monomethine Cyanine Dyes with Bacteriophage MS2: A Fluorescence Study. *J. Mol. Liq.* **2020,** *302*, 112569. DOI:10.1016/j.molliq.2020.112569

22. Waterborg, J. H.; Matthews, H. R. The Lowry Method for Protein Quantitation. *Methods Mol. Biol.* **1984**, *1*, 1–3. DOI:10.1007/978-1-59745-198-7_2

23. Delgado, A. V.; González-Caballero, F.; Hunter, R. J.; Koopal, L. K.; Lyklema, J. Measurement and Interpretation of Electrokinetic Phenomena. *J. Coll. Int. Sci.* **2007**, *309*, 194–224. DOI:10.1016/j.jcis.2006.12.075

24. Stetefeld, J.; McKenna, S.A.; Patel, T.R. Dynamic Light Scattering: a Practical Guide and Applications in Biomedical Sciences. *Biophys Rev*. **2016**. *8*(4), 409-427. DOI: 10.1007/s12551-016-0218-6

25. Farafonov, V. S.; Stich, M.; Nerukh, D. Reconstruction and Validation of Entire Virus Model with Complete Genome from Mixed Resolution Cryo-EM Density. *Faraday Discuss.* **2022**, accepted. DOI:10.1039/D2FD00053A